Study on Growth-inhibitory Mechanism of Petit-High Pressure Carbon Dioxide Pasteurization Technology

Study on Growth-inhibitory Mechanism of *Petit*-High Pressure Carbon Dioxide Pasteurization Technology

（微高圧二酸化炭素ガス殺菌技術の増殖阻害メカニズムに関する研究）

2016

The United Graduate School of Agricultural Sciences, Gifu University

Science of Biological Resources

(Gifu University)

NIU LIYUAN

Study on Growth-inhibitory Mechanism of *Petit*-High Pressure Carbon Dioxide Pasteurization Technology

（微高圧二酸化炭素ガス殺菌技術の増殖阻害メカニズムに関する研究）

NIU LIYUAN

Contents

1. INTRODUCTION

1.1 Nonthermal processing technology of foods

Thermal processing is the most well-known and old technology for inactivating undesirable microorganisms in foods. Heat destroys microbial pathogens and spoilage organisms. However, it is difficult to balance over-heating and under-heating. Over-processing makes many negative effects on foods: destruction of thermolabile vitamin, particular thiamine, vitamin C and folate and decrease of organoleptic quality [1]. As a result, nonthermal processing technologies have been proposed in the last few years and currently being explored on a global scale. Among nonthermal technologies, High Hydrostatic Pressure (HHP), Pulsed Electric Fields (PEF) and high intensity ultra sound combined with pressure are the most extensively researched ones [2]. Especially HHP is the envisaged as a promising processing technique to improve microbial safety of food products while preserving nutritional and sensory characteristics.

High Pressure Carbon Dioxide (HPCD) as an alternative has also aroused high interest in the last years. The inhibitory effect of carbon dioxide (CO_2) on bacteria growth was first discovered in 1927 in Yale University [3]. In 1951, CO_2 used as a pasteurized agent was addressed by Fraser [4]. He collected the contents of *Escherichia coli* by busting cells in liquid culture with a sudden release of pressurized (1.7 MPa-6.2 MPa) gases (argon, nitrogen, nitric oxide and CO_2) at 37℃ and found that the other three gases were less effective than CO_2. Since then, either subcritical or supercritical CO_2 has been of interest to more and more investigators in the field of food processing. Over other gases, carbon dioxide is nontoxic, inert in most situations, inexpensive, readily available and potent bactericidal action, which make it as a

potent pasteurized agent [5].

1.2 *Petit*-High Pressure Carbon Dioxide (*p*-HPCD) technology

HPCD technique has many important opportunities in food processing industry: natural image; high fresh-like organoleptic quality; continuous processing for liquid foods, etc. In addition, the pressure used in HPCD (generally < 20 MPa) is greatly lower than that employed in HHP (300 MPa ~ 600 MPa) [6]. Although application of HPCD in food preservation makes the processing more economical and easier to handle, researchers never stop exploring other possibilities.

Petit-High Pressure Carbon Dioxide (*p*-HPCD) pasteurization method, the pressure level of which is generally 1.5 atm ~ 13 atm, was first introduced by Nobuyoshi Harada et al. in 2008 [7]. They pasteurized Lyceum Barbarum fruit juice harvested from China by carbon dioxide gas under mild to high pressure (3 atm to 50 atm) for 1 day to 14 days at room temperature. Surprisingly, pasteurized effect on microorganisms of *p*-HPCD with long time treatment (3 atm, room temperature, 7d) was similar to the effect of HPCD with short time treatment (50 atm, room temperature, one day). Both treatments showed significantly pasteurized effects on bacteria, yeast and mold. *P*-HPCD with long time treatment seems a more promising pasteurization technique. This new technique is applicable in not only food processing but also food distribution including storage and transport. On the one hand, relative to refrigeration, the common storage method, *p*-HPCD applied in storage has better effects on inhibiting microorganism growth. On the other hand, because pressure level during transport is restricted to be less than 4 atm in Japan, it is realistic for food transport under *p*-HPCD condition. In 2009, a patent (JP2009077702 (A)) was granted in Japan for the new pasteurization method called as carbon dioxide microhyperbaric long period treatment.

1.3 Hypotheses on mechanism of CO_2 bactericidal action

A few investigators also applied some other gases to reduce viable microbial counts. Compared to these gases under high pressure including nitrogen (N_2), argon (Ar), nitrous oxide (N_2O), oxygen (O_2) and tetrafluoroethane (TFE), HPCD in general results in greater microbial inactivation [6]. Dillow et al. [8] pointed out the importance of proximity to the critical point and chemical properties on inactivation effectiveness. Because the experimental conditions were well removed from the critical point of N_2 (T_c = –147℃; P_c = 3.39 MPa) and Ar (T_c = –122.28℃; P_c = 4.90 MPa), both gases did not exhibit the special gas-like mass transport properties and liquid-like densities of a supercritical fluid. With respect to TFE (T_c = –55℃; P_c = 4.06 MPa) and N_2O (T_c = 36.5℃; P_c = 7.25 MPa), it has critical points similar to CO_2 (T_c = 30.98℃; P_c = 7.37 MPa), but different chemical properties (dipole moment, D_{CO_2} = 0, D_{TFE} = 1.80±0.22D; solubility parameter, δ_{CO_2} = 7.0, δ_{TFE} = 13.6).

In recent years, many investigations have focused on the mechanism of CO_2 bactericidal action. Based on physical and chemical properties of CO_2, there are two general mechanisms presumed and discussed: mechanical cell rupture and physiological deactivation. The mechanism of cell rupture was the earliest presumed and supported by microscopy image of burst cells during pressurization stage [4, 9, 10]. Burst cells, wrinkles and holes on the cell surface have been observed using scanning electron microscope [11]. The physiological deactivation mechanism involves several theories, such as (1) decrease of intracellular pH (pHi), (2) cell membrane modification, (3) key enzyme inactivation due to pHi lowering, (4) direct (indirect) effect of molecular HCO_3^- and CO_3^{2-} on metabolism, (5) extraction of cell contents [5, 6]. However, most of these researches were conducted under high-pressure condition even supercritical

condition, while pressure employed in *p*-HPCD is far from the critical point of CO_2. Physical properties of CO_2, such as density, diffusivity, solubility in aqueous solution and extraction power, vary with pressure and temperature [12]; it is difficult to say whether these theories above also can account for *p*-HPCD pasteurization mechanism.

1.4 Purpose in this study

Because of advantages mentioned above, *p*-HPCD technology could be one of the most available nonthermal pasteurization technologies in some years. However, without provision of clear, objective and convincing data on this new technique, its rapid development will be hindered in food processing and distribution. In this study, we analyze biological effects of *p*-HPCD on the transcription level of yeast *Saccharomyces cerevisiae* and try to elucidate the growth-inhibitory mechanism of *p*-HPCD stress through functional genomics and metabolomics approaches.

Changes in gene expression profiles indicate changes in physiological conditions [13]. Organisms respond to stressful conditions by initiating a program of adaptive transcriptional responses, as described for the environmental stress response (ESR) whose goal appears to minimize cell damage [14]. Functional genomics approach was used in this study to extract meaningful information from microarray analyses. Altered genes were categorized by localization of gene products and their functions through Munich Information Centre for Protein Sequences (MIPS, http://mips.gsf.de/funcatDB/). MIPS focuses on genome oriented bioinformatics research and supports a set of generic databases as well as the systematic comparative analysis of microbial, fungal, and plant genomes. While mRNA gene expression data analysis does not tell the whole story of what might be happening in a cell, metabolic profiling can give an instantaneous snapshot of the physiology of that cell [15]. In this study, we used capillary electrophoresis-time-of flight mass spectrometry (CE-TOFMS) to analyze a wide variety of metabolite responses to *p*-HPCD stress in yeast. The combination of genomics and metabolomics provides a better understanding on cellular responses to *p*-HPCD stress.

2. MATERIALS AND METHODS

2.1 Strain and growth conditions

Yeast *Saccharomyces cerevisiae* S288C (*MATα SUC2 mal mel gal2 CUP1*) preserved in -80°C freezer was inoculated into yeast extract/ peptone/dextrose medium (YPD) (2% polypeptone, 1% yeast extract, 2% glucose) medium, and cultivated at 100 rpm (revolutions per minute) agitation and 25°C for 2~3 days. Then yeast culture was diluted (100-fold) into fresh YPD medium in sterile tube sealed with silicone sponge tapered plug and cultivated under the same condition to resume growth to logarithm phase (OD_{600} = 0.5 ~ 0.8).

2.2 *Petit*-High Pressure Carbon Dioxide (*p*-HPCD) treatment

After cultivation, yeast culture in sterile tube sealed with silicone sponge tapered plug was transferred to a high-pressure vessel (30-11HF4, High Pressure Equipment, Elie, PA, USA), which was placed in a 25°C thermostatic bath, and incubated under 0.5 MPa, 0.7 MPa and 0.9 MPa of CO_2 for 2 h, respectively. Yeast culture kept in thermostatic bath without treatment (0.1 MPa) was used as a control. After *p*-HPCD treatment, cells were harvested by centrifugation and pellets were preserved in freezer at –80°C as soon as possible for taking good-quality RNA. Meanwhile, colony-forming units (CFU) were monitored before and after treatment. Yeast cells treated by condition that causes 50% decrease of specific growth rate (SGR) were selected to analyze transcriptional effects of *p*-HPCD stress. Specific growth rate (SGR) was calculated by $(\mathrm{Ln}\ N_1 - \mathrm{Ln}\ N_0) / t$ (N_0: number of cells before treatment; N_1: number of cells after treatment or cultivation; t: treatment time).

2.3 RNA preparation and DNA microarray data analysis

Yeast cells grown in YPD medium at 25℃ to logarithmic phase were treated by 0.5 MPa of CO_2 for 2 h at 25℃ and then harvested. Total RNA was extracted from1 ml of *p*-HPCD-treated or non-treated yeast cells using the Fast RNA®Pro Red Kit (MP Biomedicals, CA, USA) and RNeasy® Mini Kit (QIAGEN Co. Ltd., USA) following the manufacturer's instructions. The quantity and quality of extracted RNA were detected by NanoDrop (SCRUM Co. Ltd., Japan). RNA with high purification that OD_{260}/D_{280} is 1.8 ~ 2.0 was used in our study.

DNA microarray was carried as per biological experiments reported by Matsuoka et al. [16]. Poly(A)+ RNA was purified from total RNA with an Oligotex-dT30 mRNA purification kit (Takara, Otsu, Japan). Fluorescently labeled cDNA was synthesized by oligo dT-primer polymerization using PowerScript™ reverse transcriptase. Cycle DNA obtained from poly(A)+ RNA of control was fluorescently labeled with Cy3-UTP and cDNA made from *p*-HPCD treated sample was fluorescently labeled with Cy5-UTP. The two labeled cDNA pools were mixed and hybridized with a yeast DNA chip (DNA Chip Research, Inc., Yokohama, Japan) for 24~36 h at 65℃. After hybridization, the DNA chips were washed, dried and scanned with a confocal laser ScanArray 4000 (GSI Lumonics, Billerica, MA, USA) system. The image data was quantitated using the QuantArray Quantitative Microarray Analysis application program (GSI Lumonics, Billerica, MA, USA). The fluorescence intensity of each spot on the image was subtracted from the background, and the ratios of intensity Cy5/Cy3 were calculated and normalized with a median value of the GeneSpring software (Silicon Genetics, Red Wood, CA, USA) as a positive control. Normalized data ratios >2-fold or <0.5-fold between treatment and control were considered up- or

down-regulated, respectively. In this study, Student's *t*-test as a statistical filter was carried out. The *p*-value < 0.05 was considered statistically significant.

2.4 Cluster analysis

In order to acquire more meaningful information from the large numbers of data generated from DNA microarrays, we carried out hierarchical cluster analysis using GeneSpring software to explore the changes of transcriptional patterns in response to *p*-HPCD stress. Genes altered by *p*-HPCD were compared to genes altered by other various stresses including herbicides, detergents, food additives and gases combined with changes of temperature and pressure. The hierarchical clustering was constructed on the base of 5,940 open reading frames. The settings for the calculations were as follows: the similarity was measured by standard correlation; the separation ratio was 1.0; and the minimum distance was 0.001.

2.5 Reverse-transcriptional PCR

Reverse transcriptase-polymerase chain reaction (RT-PCR) was performed using the ReverTra Ace® qPCR RT Master Mix (TOYOBO, Osaka, Japan) for preparing a cDNA libraries solution following the PCR step. The reverse transcription conditions were: 37°C for 15 min, 50°C for 5 min and 98°C for 5 min. Then the reacted solution was stored at 4°C (can be used directly) or -20°C. The PCR was performed using a 10-fold dilution of cDNA libraries solution and the Go-Taq Green (Promega Corporation, WI, USA). PCR conditions were: 95°C for 2 min, 25 cycles of 95°C 1 min, 57°C 1 min, and 72°C 2 min, and a final 72°C for 4 min. The PCR primers were all designed with the available GenBank sequence data and the Primer3Plus web interface (http://primer3plus.com/cgi-bin/dev/primer3plus.cgi) (Table 1). Independent RT-PCR experiment was performed at least three times for individual gene to achieve and convince the reproducibility of selected genes and their expressions.

Table 1. Primers used in this study.

Gene	Forward primer	Reverse primer
ACT1	5'-ATTGCCGAAAGAATGCAAAAGG-3'	5'-CGCACAAAAGCAGAGATTAGAAACA-3'
CAR2	5'-CACGCAGAAGATTTCGTCCCT-3'	5'-ACAGAACACATGAGACGGGAA-3'
DUR1, 2	5'-TACGCACTATTAGAGTTGGCTA-3'	5'-TACCTTTGGCTTTGTAACCAG-3'
CAR1	5'-ACAGATTCCCCTTGACCTTG-3'	5'-ACACCATCGACGTCATAGGA-3'
ARG4	5'-TTACAATGCGTCTCTTCCGTA-3'	5'-CATCTAATAGGTTGTGCCCTT-3'
ARG1	5'-GCCGCATCCAACTTAGCAA-3'	5'-CGGTCAACTCATCCATAGAGG-3'
ARG3	5'-TGTATTTTTGCCCGTGTGAA-3'	5'-GTTTCAGCTTGGCCTGTTTC-3'
CPA1	5'-GCTGTTGAATCTCTGGCACA-3'	5'-CGTCGAATTCAGAAGCAACA-3'
CPA2	5'-TACATCAACAGAGCCTACGAA-3'	5'-CAGATGCGAAAAGATCCCT-3'
MET3	5'-GCCCTTTTCCAAGATGATGA-3'	5'-CTGGATGTTCTGGGTCACCT-3'
MET16	5'-ATTTGGTTTGACTGGCTTGG-3'	5'-ATCTGCCTCCGATTCACATC-3'
MET10	5'-TACCACCATCTCCAAAGCAAC-3'	5'-CCAAGTAGGGCCACACAAGTA-3'
MET17	5'-CGCTCAAACCCTTGCCATCCA-3'	5'-TGACAGAAGTAACCACCGGCACCA-3'
MET6	5'-CGGCCAAAAGCCAGTTGACGA-3'	5'-GCAACTGGCAAGCCCTTGATGG-3'
SAM2	5'-CAGATATCGCTCAAGGTCTGC-3'	5'-GGTAACCCTTCTGGAGTTTCG-3'
OPI3	5'-TGGGGCCAGAAAGGGCTGTT-3'	5'-AGCCCCGCAGGCTTTCCTTT-3'

2.6 Metabolites extraction and metabolomic analysis

Metabolites were extracted according to the study protocol that was provided by Human Metabolomics Technologies Inc. (HMT, Tsuruoka, Yamagata, Japan). Yeast cells were treated by 0.5 MPa of CO_2 at 25℃ for 2 h and OD_{600} was measured after treatment. Cells without *p*-HPCD treatment was used as a control. The culture volume used in the metabolomic analysis was calculated using this formula: Sampling volume (ml) = $10/OD_{600}$. About 10^8 of yeast cells were required for metabolomic analysis. The sample with required volume was filtered by using a suction-filtering system equipped with an HTTP 0.4 μm pore filter (47 mm diameter Isopore Membrane Filter, Millipore, Billerica, MA, USA). Cells trapped on the filter were washed twice by Milli-Q water and then soaked in 2 ml of methanol (MS analysis grade, Wako Pure Chemical Industries, Osaka, Japan) and 5 μM internal standard (provided by HMT) in an encapsulated plastic dish. After 1 min, the dish was sonicated for 30 s to suspend the cells completely, and then 1.6 ml of the methanol solution together with the cells was transferred to a 15 ml centrifugation tube (Corning Incorporated, Corning, NY, USA). Then 1600 μl of chloroform and 640 μl of Milli-Q water were added to the solution. The mixed solution was then centrifuged at 2300 g for 5 min at 4°C. The supernatant was transferred to an Amicon Ultrafree MC filter unit (Millipore) and centrifuged at 9100 g for 120 min at 4°C to remove proteins. Lastly, filtrates were dissolved in 50 μl of Milli-Q water.

CE-TOFMS analysis was performed using an Agilent CE-TOFMS system (Agilent Technologies, Santa Clara, CA, USA). Cationic metabolites were separated through a fused silica capillary (50μm i.d. × 80 cm total length) preconditioned with a commercial buffer solution (H3301-1001, HMT), and a commercial sheath liquid

(H3301-1020, HMT) was delivered. Sample solution was injected at 50 mbar for 10 s and a positive voltage of 27 kV was used. Electrospray ionization-mass spectrometry (ESI-MS) was conducted in the positive mode and the capillary voltage was set at 4000 V. Anionic metabolites were also analyzed through the fused silica capillary preconditioned with a commercial buffer solution (H3302-1021, HMT), and the same solution was injected at 50 mbar for 25 s and a positive voltage of 30 kV was applied. ESI-MS was conducted in the negative mode, and the capillary voltage was set at 3500 V. The exact mass data were obtained over a 50−1000 m/z range. Obtained data were then preprocessed using the automatic integration software MasterHands ver.2.13.0.8.h (developed by Keio University). Each metabolite was detected based on the peak information including m/z, migration time and peak area. The relative peak area was calculated as the ratio of peak area of target metabolite to product of peak area of internal standard and cell number.

2.7 Thin layer chromatography

Total lipids from yeast cells were extracted according to a modification of the protocol described by Bligh & Dyer method [17]. Yeast cells were grown in YPD medium to exponential phase (OD_{600} = 0.5 ~ 0.8), and then treated by 0.5 MPa of CO_2 at 25℃. Yeast cells were harvested after 0 h, 2 h and 4 h treatment and frozen immediately in liquid nitrogen. CFU was counted at each time point. The frozen pellet was resuspended in 1.6 ml ice-cold distilled H_2O. Total lipids were extracted with 6 ml of chloroform and methanol (1:2) mix and 0.8 ml glass beads. The ratio of chloroform-methanol-H_2O was 1:2:0.8 (v/v). Then chloroform and distilled H_2O were added, and the ratio of all three became 2:2:1.8 (v/v). The cell pellet was separated from liquid phase by thorough centrifugation. The entire liquid phase was collected. Then 3.2 ml of chloroform was added to the cell pellet and resuspended. After centrifugation, supernatant was added to liquid phase collected before. The organic and aqueous phases were separated by centrifugation. The chloroform layer was recovered, evaporated to dryness under nitrogen gas, and then resuspended in chloroform to give the total lipid sample.

Extracted lipids corresponding to 5.2×10^7 yeast cells of each sample were analyzed by thin layer chromatography using Silica Gel 60 (Merck; 20 × 20 cm). The silica gel plates were developed with a chloroform/methanol/acetic acid/water (65:32:2:3, v/v) solvent system for ~60 min at room temperature and air-dried for about 30 min. The plates were then sprayed with 12% (v/v) H_2SO_4, 2% $CuSO_4$ and placed on a hot plate at 120 ℃ for 10 min. Phosphatidylcholine (PC) and phosphatidylethanolamine (PE) from egg yolk, and phosphatidylinositol (PI) from soybean (Sigma-Aldrich Co. LLC, Tokyo, Japan) were used as standards.

2.8 Scanning Electron Microscopy

The pellets of the centrifuged cell suspensions including untreated and treated with CO_2 under pressures of 0.5 MPa, 1.0 MPa, 2.0 MPa and 4.0 MPa at 25℃,were first pre-fixed for 2 h in a 2.0% (v/v) Glutaraldehyde prepared in 0.1 M phosphate buffer (pH 7.2), and then rinsed with 0.1 M phosphate buffer (pH 7.2) for three times. The post-fixation was performed for 2 h in a 1% OsO_4 sodium cacodylate buffer (pH 7.2). After all fixations, the pellets were dehydrated in an aqueous ethanol solution series (50%, 70%, 80%, 90%, 95%, 99.5%, 100%, v/v), treated each sample with tert-Butyl alcohol three times, freeze-dried (ES-2030, Hitachi, Ltd., Japan), and coated with gold-palladium (E-1010, Hitachi, Ltd., Japan). Inspection and photomicrographs were conducted with a scanning electron microscope (FE-SEM, S-4700, Hitachi, Ltd., Japan) operated at a voltage of 1.5 kV.

3. RESULTS

3.1 Conditions for treatment with *p*-HPCD

Cell physiology cannot be affected significantly under weak stress conditions, whereas it is difficult to extract sufficient mRNA from cells under lethal conditions. With reference to previous reports, we can expect adequate stress responses under a treatment condition that causes about 50% growth inhibition [16]. By analyzing SGR of yeast cells under different treatment conditions, we found that under condition of 0.5 MPa of CO_2 at 25°C, SGR was decreased by about 50% (Fig. 1), and consequently sequent experiments were performed under this condition.

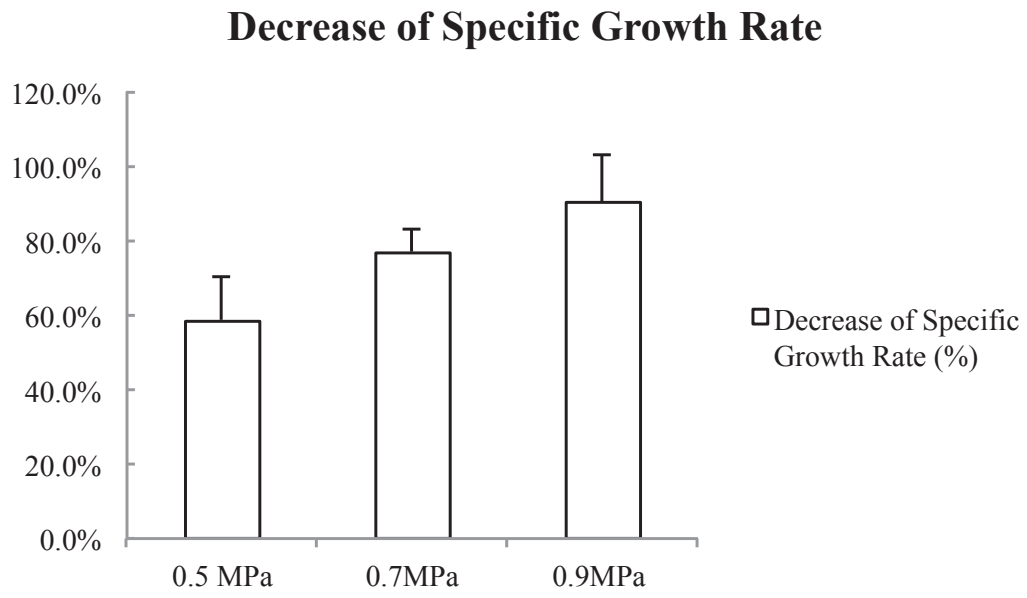

Fig. 1. Growth inhibition of *p*-HPCD on yeast was showed by decrease of specific growth rate (SGR).

3.2 Effects of *p*-HPCD stress on genome-wide transcription in yeast

After global normalization, we removed the spots with a Cy5 intensity of less than 4,000 because of the doubtful results of lower intensity. Given that more than 99% of the control spots without DNA had intensities lower than 1,000 for Cy3, the cutoff line for precluding negative results was taken as a scanned intensity below 2,000 for Cy3 (which corresponded to an intensity of 4,000 for Cy5). Results between 1,000 and 2,000 of intensity for Cy3 were considered doubtful, and therefore discarded [16]. To identify genes demonstrating a maximal labor-associated change in expression, the *p*-value of each gene was calculated by student's *t*-test. This *p*-value was used as a measure of the magnitude of the change and inter-subject variability rather than to determine significance. Finally, we selected a total of 5,940 genes from 6,335 spots and from these 5,940 genes we selected 476 as the up-regulated genes and 361 as the down-regulated genes, by pressure treatment. The 476 induced genes were selected as the genes with Cy5 intensity two-fold higher than Cy3 intensity as well as *p*-values less than 0.05. The 361 down-regulated genes were also selected as the genes with Cy5 intensity 0.5-fold lower than Cy3 intensity as well as *p*-values less than 0.05.

3.3 Clustering of genome-wide expression patterns in yeast

The expression data of DNA microarray were then categorized by localization of gene products and by functions according to accepted gene ontologies through MIPS database (Fig. 2). The clustering profiles reveal the transcriptional responses of yeast to *p*-HPCD stress. By ordering *p*-values obtained from MIPS database (*p*-value < 0.05 was considered significant) of functional categories, “cell rescue, defense and virulence” and “metabolism” were found highly significant. Yeast cell seems to regulate cellular processes to minimize cell damage and adapt to the environment change. On the other hand, functional categories of down-regulated genes included “protein synthesis”, “transcription”, and “protein with binding function or cofactor requirement (structural and catalytic)”. It appears that the yeast was slowing or halting growth to conserve mass and energy for survival. The categories whose *p*-values (hypergeometric distribution) less than 0.05 and the percentage of selected genes within each category are listed in Table 2.

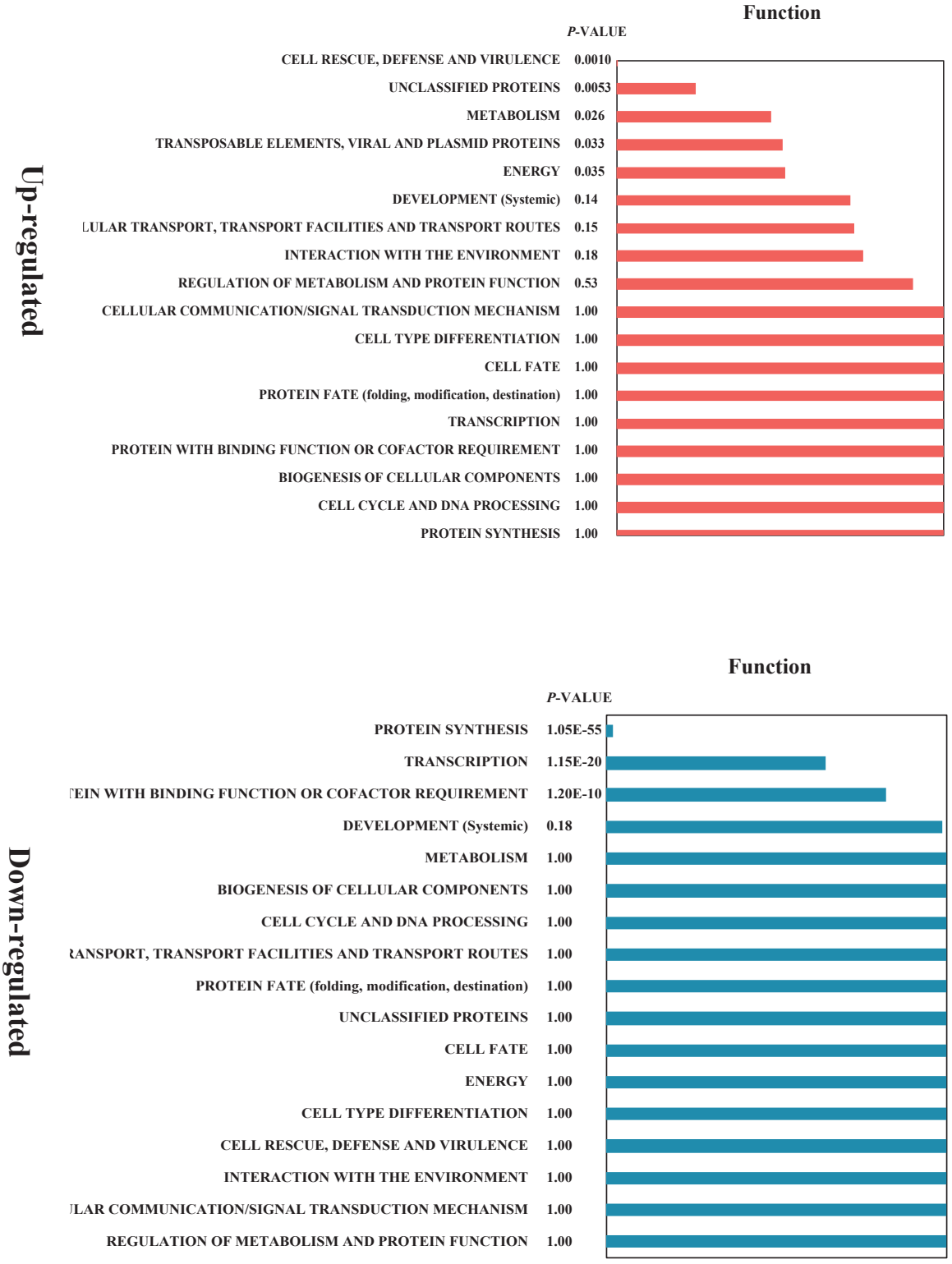

Fig. 2. Up-regulated (red) and down-regulated (blue) ORFs (open reading frames) in response to treatment with *p*-HPCD. ORFs are classified into MIPS categories of function and localization of gene products.

Table 2. MIPS functional classification of altered ORFs in response to *p*-HPCD stress.

Up-regulated Function	***p*-value**	**Percent (%)**
Cell Rescue, Defense and Virulence	0.0010	11.01%
Unclassified Proteins	0.0053	9.12%
Metabolism	0.026	8.65%
Transposable Elements, Viral and Plasmid Proteins	0.033	12.50%
Energy	0.035	10.08%
Down-regulated Function	***p*-value**	**Percent (%)**
Protein Synthesis	1.05E-55	25.83%
Transcription	1.15E-20	11.98%
Protein with Binding Function or Cofactor Requirement	1.20E-10	9.91%

In order to further understand the changes in expression profiles, up- and down-regulated genes were classified into subcategories based upon function of gene product. Subcategories of top two significantly induced categories “cell rescue, defense and virulence” and “metabolism” are listed in Table 3. “Cell rescue, defense and virulence” category was characterized by remarkably induced subcategories “stress response”, “disease, virulence and defense” and “detoxification”. Moreover, genes within “amino acid metabolism”, “nitrogen, sulfur and selenium metabolism”, and “metabolism of vitamins, cofactors, and prosthetic groups” functional subcategories were found highly induced. Induced genes within these significantly induced subcategories are listed in Table 4.

Table 3. The top two significant categories (p-value < 0.05) and their subcategories after p-HPCD treatment.

Up-regulated Function		
CELL RESCUE, DEFENSE AND VIRULENCE		
Subcategory	p-value	Percent (%)
Stress response	0.011	10.44%
Disease, virulence and defense	0.013	20.00%
Detoxification	0.00097	16.24%
METABOLISM		
Subcategory	p-value	Percent (%)
Amino acid metabolism	0.0021	12.76%
Nitrogen, sulfur and selenium metabolism	6.6E-06	21.65%
Nucleotide/nucleoside/nucleobase metabolism	0.53	7.69%
Phosphate metabolism	0.41	8.04%
C-compound and carbohydrate metabolism	1.0	6.22%
Lipid, fatty acid and isoprenoid metabolism	0.064	9.31%
Secondary metabolism	1.0	5.59%
Metabolism of vitamins, cofactors, and prosthetic groups	0.0023	14.02%

Table 4. Induced genes within significantly induced subcategories after *p*-HPCD treatment.

Function								
CELL RESCUE, DEFENSE AND VIRULENCE								
Subcategory	Gene name							
Stress response	*DDR2*	*DDR48*	*GAC1*	*AHP1*	*YGP1*	*XBP1*	*GCY1*	*UGA2*
	SNZ1	*ORM2*	*HSP26*	*SNO1*	*HOR7*	*TRX2*	*CIN5*	*SDP1*
	GPD1	*PAI3*	*SPL2*	*UBC5*	*MRK1*	*YRO2*	*HSF1*	*SNO4*
	ATH1	*CYC7*	*SIP18*	*WSC3*	*GTT2*	*GRE2*	*PHO5*	*AGP2*
	GRX1	*GRE1*	*SOD1*	*YKR049c*	*YJL144w*	*HAC1*	*PEP4*	*VRP1*
	SML1	*STF2*	*GPX1*	*HSP31*	*HMF1*	*TTR1*	*MPT5*	
Disease, virulence and defense	*FET3*	*CIN5*	*MLF3*	*LAP3*	*CUP1-2*	*PDR3*	*CUP1-1*	
Detoxification	*SIT1*	*HMX1*	*CRS5*	*ENB1*	*AHP1*	*ARN1*	*TRX2*	*GTT2*
	GRE2	*GRX1*	*SOD1*	*ARN2*	*LAP3*	*CUP1-2*	*GPX1*	*YFR022w*
	PDR3	*CUP1-1*	*TTR1*					
METABOLISM								
Subcategory	Gene name							
Amino acid metabolism	*CAR2*	*MET17*	*MET13*	*YHR033w*	*DUR1,2*	*CAR1*	*GDH1*	*CHA1*
	UGA2	*BNA1*	*IDP1*	*ILV6*	*MET6*	*ECM38*	*STR3*	*LYS5*
	UGA1	*MMF1*	*YMR226c*	*ALT1*	*ARG4*	*PUT1*	*ARO8*	*MET3*
	CIT2	*MET28*	*LYS1*	*GDH2*	*MUP3*	*MET10*	*CPA2*	
Nitrogen, sulfur and selenium metabolism	*CAR2*	*FUN34*	*MET17*	*MET13*	*DUR1,2*	*CAR1*	*GAT1*	*YOL153c*
	GDH1	*ADY2*	*DAL80*	*DAL3*	*CPS1*	*STR3*	*UGA1*	*ALT1*
	UGA4	*MET3*	*MET28*	*GDH2*	*MET10*			
Metabolism of vitamins, cofactors,	*HMX1*	*MET13*	*DIA3*	*YEL041w*	*SNZ1*	*SNO1*	*BNA1*	*PHO12*
and prosthetic groups	*PYC1*	*ECM38*	*LYS5*	*BIO5*	*SNO4*	*PHO11*	*RIB5*	*GTT2*
	GRE2	*PHO5*	*ARN2*	*PNC1*	*ARI1*	*ACS1*	*PYC2*	

Note: Genes marked in red and black are annotated and uncharacterized, respectively. Genes classified into subcategories of function are listed left to right in descending order of induction level.

3.4 Genes related to urea cycle were induced in response to *p*-HPCD stress

"Nitrogen, sulfur and selenium metabolism", "detoxification", and "amino acid metabolism" were the top three significant subcategories within all subcategories of the most significant categories "cell rescue, defense and virulence" and "metabolism" (Table 3). Also they were further classified into subcategories as well (Table 5). Among these significant subcategories, "metabolism of urea cycle" possessed the smallest *p*-value 0.00041. Even within all the significant subcategories, it was also the most significant statistically. Furthermore, 67% of genes associated with urea metabolism were found highly up-regulated (Table 6). RT-PCR was performed on these genes (*CAR2*, *DUR1,2*, *CAR1*, *ARG4*, *ARG3* and *ARG1*) related to urea cycle metabolism. *ARG4* encodes arginosuccinate lyase, a cytosolic enzyme that catalyzes the final step in arginine biosynthesis. Arginase encoded by *CAR1* gene, catabolizes arginine to ornithine and urea. Although *CAR2* and *DUR1,2* genes do not directly participate in metabolism of urea cycle, expression of both genes are increased by the presence of allophanate, a degradation of urea [18, 19]. *ACT1* gene was used as the reference gene, because its expression level in response to *p*-HPCD stress was found stable. The RT-PCR results correlated with the DNA microarray data (Fig. 3). Thus, the effect of *p*-HPCD treatment to metabolism of urea cycle was confirmed.

Table 5. The top three significant subcategories within all subcategories of the most significant categories "cell rescue, defense and virulence" and "metabolism".

Up-regulated function		
Nitrogen, sulfur and selenium metabolism		
Subcategory	*p*-value	Percent (%)
ND		
Detoxification		
Subcategory	*p*-value	Percent (%)
Detoxification by modification	0.0017	50.00%
Oxygen and radical detoxification	0.00043	30.77%
Glutathione conjugation reaction	0.0037	60.00%
Peroxidase reaction	0.00090	57.14%
Amino acid metabolism		
Subcategory	*p*-value	Percent (%)
Assimilation of ammonia, metabolism of the glutamate group	0.0021	21.28%
Metabolism of glutamate	0.0057	26.09%
Metabolism of arginine	0.017	23.81%
Metabolism of urea cycle, creatine and polyamines	0.022	26.67%
Metabolism of urea (urea cycle)	0.00041	66.67%
Metabolism of the aspartate family	0.024	15.15%
Metabolism of methionine	0.043	17.14%

Table 6. List of genes associated with metabolism of urea cycle categorized by MIPS database.

Gene Name	Ratio	*p*-value	Function
CAR2	5.6	0.00011	Ornithine aminotransferase
DUR1,2	4.4	0.0000062	Urea amidolyase
CAR1	4.2	0.000029	Arginase
ARG4	2.5	0.0000090	Arginosuccinate lyase
ARG1	1.2	0.32	Argininosuccinate synthetase
ARG3	0.7	0.013	Ornithine carbamoyltransferase

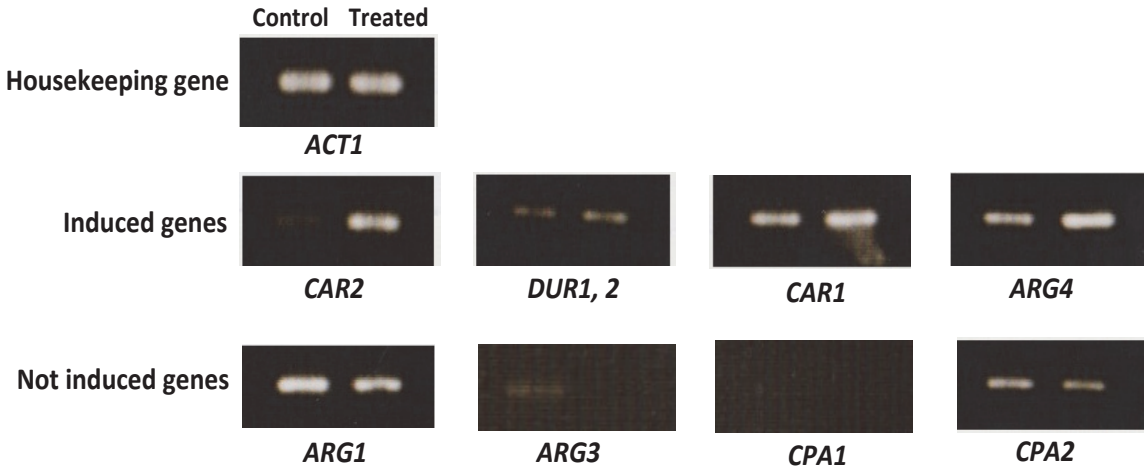

Fig. 3. RT-PCR results of genes involved in the urea cycle pathway are compared between treatment and control (without treatment).

3.5 Clustering analysis of ORFs responding to *p*-HPCD and other stresses

In order to acquire more meaningful information from the large numbers of data generated from DNA microarrays, ORFs in response to *p*-HPCD stress was compared with other stresses. As shown in Fig. 4, CO_2 pressure is grouped into a cluster including Sodium Dodecyl Sulfate (SDS) and Roundup. SDS is a surfactant that helps to reduce surface tension of the water and mainly used in detergents for laundry with many cleaning applications [20]. Roundup is a commercial herbicides product containing glyphosate as the active ingredient and detergents as stabilizer of glyphosate [21].

Detergents are common amphiphilic substances that possess both polar and non-polar moieties and have hydrophobic and hydrophilic portions. They are widely used to solubilize proteins out of cell membranes although the sensitivity of proteins to detergents is different [22]. Additionally, detergents can replace part or all of the original lipid molecules around the membrane proteins to form protein-detergent complexes, which are soluble in aqueous solutions [22]. Detergents disorder membranes structurally and functionally, even lead to rupture or lysis. This hierarchical clustering result gives a useful hint that cell membrane may be an important target of *p*-HPCD stress to lead to cell growth inhibition.

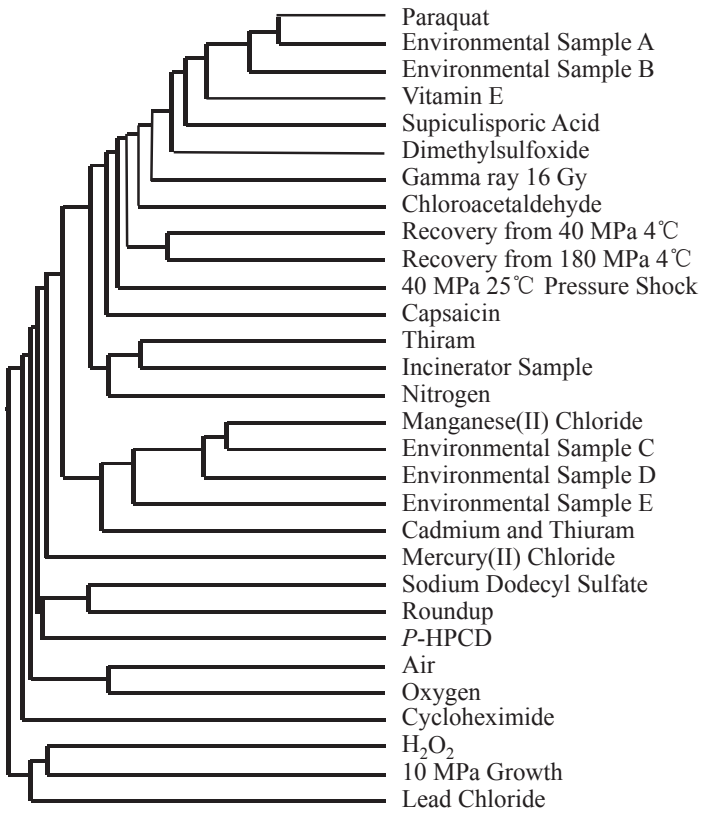

Fig. 4. Hierarchical clustering analysis. The hierarchical clustering was performed using GeneSpring. ORFs altered by *p*-HPCD stress were compared with ORFs altered in response to other stresses that are deposited to Gene Expression Omnibus (GEO, https://www.ncbi.nlm.nih.gov/geo/). The length of the branch to the node indicates the degree of similarity between different stresses based on each expression profile. The treatment conditions are as following: Paraquat (35 ppm,2 h), Environmental waters A-E (100%, 2 h), Vitamin E (saturate, 2 h), Supiculisporic Acid (0.16%, 2 h), Dimethylsulfoxide (10%, 2 h), Gamma ray (16 Gy, 2 h), Chloroacetaldehyde (25 ppm,2 h), Lethal pressure 1 (after 40 MPa 4℃ 12 h, recovery for 60 min), Lethal pressure 2 (after 180 MPa 4℃ 0 min, recovery for 60 min), Pressure shock (40 MPa 25℃, 2 h), Capsaicin (250 ppm, 2 h), Thiram (5 uM, 2 h), Nitrogen (40 MPa, 2 h), Manganese Chloride (5 mM, 2 h), Cadmium and Thiram (10 μM and 2.5 μM, 2 h), Mercury (II) Chloride (0.7 mM, 2 h), Sodium dodecyl sulfate (0.01%,2 h), Roundup hi-load (×1,500 dilution, 2 h), *P*-HPCD (0.5 MPa, 2 h), Air (10 MPa, 2 h), Oxygen (0.5 MPa, 2 h), Cycloheximide (15 μM, 2 h), Hydrogen peroxide (10 mM, 2 h), Growth under pressure (10 MPa, 25℃, 16 h), Lead Chloride (2 mM, 2 h).

3.6 Metabolites involving urea cycle were increased after *p*-HPCD treatment

The metabolite responses to *p*-HPCD stress was determined by extracting and measuring metabolites in *Saccharomyces cerevisiae* S288C strain after treatment for 1 h and 2 h, respectively. In the CE-TOFMS analysis, 284 metabolites including 170 cations and 114 anions were detected.

Through DNA microarray data and RT-PCR experiment, we confirmed that genes (*CAR2*, *DUR1,2*, *CAR1* and *ARG4*) related to metabolism of urea cycle were highly up-regulated by *p*-HPCD stress. Therefore, in the CE-TOFMS analysis, we investigated response of metabolites involved in urea cycle to *p*-HPCD stress. Table 7 shows the changes in related metabolites of cells with 1 h and 2 h treatment relative to metabolites of non-treated cells. Metabolites directly participating in urea biosynthesis were increased after *p*-HPCD treatment, including argininosuccinic acid, citrulline, ornithine and Arginine (Arg). Especially the product urea was remarkable increased by more than 3.9-fold after 1 h treatment of *p*-HPCD. It appears that metabolism of urea cycle in yeast cell is enhanced by *p*-HPCD stress.

Table 7. Amounts and relative concentrations of metabolites related to metabolism of urea cycle after *p*-HPCD treatment for 1 h and 2 h. Relative concentration of each amino acid was calculated in comparison to control.

Metabolite Name	1 h			2 h		
	Relative peak area		Relative concentration	Relative peak area		Relative concentration
	Control	Treated	Fold-change	Control	Treated	Fold-change
Urea	0.162	0.641	3.95	0.145	0.388	2.67
Argininosuccinic acid	0.034	0.059	1.75	0.030	0.055	1.83
Citrulline	0.071	0.132	1.85	0.083	0.267	3.20
Ornithine	0.048	0.084	1.76	0.061	0.101	1.66
Arg	2.480	2.940	1.19	2.570	2.560	0.99

3.7 Phosphatidylcholine synthesis was enhanced by *p*-HPCD stress

Metabolite responses to *p*-HPCD stress were determined by extracting and measuring metabolites in yeast *Saccharomyces cerevisiae* S288C strain after treatment for 1 h and 2 h, respectively. In the CE-TOFMS analysis, 284 metabolites including 170 cations and 114 anions were detected. Among detected metabolites, there are 9 metabolites (inosine, choline, NADH, 2-isopropylmalic acid, N-ethymaleimide+H_2O, urea, 4-aminobutanoic acid (GABA), spermidine and putrescine; in descending order of increased level) increased by more than 2.5-fold after 1 h treatment, and 13 metabolites (inosine, GABA, 2-isopropylmalic acid, putrescine, pipecolic acid, spermidine, choline, adenine, NADH, nicotinamide, urea; in descending order of increased level) were increased by more than 2.5-fold after 2 h treatment.

Within these highly increased metabolites, there are several polyamine metabolites. As shown in Table 8, the relative concentration represents fold-change of each metabolite after *p*-HPCD treatment, which was calculated as the ratio of the relative peak area of target metabolite to that of control. Relative to control, GABA, spermidine and putrescine was increased by 3.32-fold, 3.09-fold and 2.88-fold after 1 h treatment and by 3.87-fold, 2.99-fold and 3.55-fold after 2 h treatment, respectively. Other related polyamine metabolites, N-Acetylputrescine and *S*-Adenosylmethionine (AdoMet), were also increased by *p*-HPCD stress (Table 8). Moreover, except spermidine, the increased extents of polyamines metabolites after treatment for 2 h were higher than those after treatment for 1 h. It is known that polyamines involve in a large number of cellular processes, such as modulation of chromatin structure, gene transcription and translation, DNA stabilization, signal transduction, cell growth and

proliferations etc. [23]. The increase of polyamines in response to *p*-HPCD stress seems to help yeast cells to better adapt to the environment change.

In addition to participate in polyamine biosynthesis, AdoMet is also involved in the methylation of proteins, RNAs, and lipids [24]. Especially AdoMet is used as a methyl donor to participate in phosphatidylcholine (PC) synthesis via phosphatidylethanolamine (PE) methylation pathway [25]. To further confirm that it is the induction of its biosynthesis, not consumption, to result in increase of AdoMet, we validate genes (*MET13*, *MET16*, *MET10*, *MET17*, *MET6* and *SAM2*) associated with AdoMet biosynthesis by RT-PCR using *ACT1* gene as the reference gene. As shown in Fig. 5, RT-PCR results are coincident with DNA microarray data. Interestingly, the key gene *OPI3* encoding phospholipid methyltransferase that catalyzes the last two steps in PE methylation pathway was also found significantly induced by *p*-HPCD stress, and its induction was confirmed by RT-PCR (Fig. 6). Moreover, through metabolomic analysis, we found level of choline and ethanolamine that participate in the other phospholipid synthesis pathway, the Kennedy pathway [26], were increased by 4.37-fold and 1.63-fold, respectively, relative to those in cell without *p*-HPCD treatment for 1h (Table 8). When treated time was prolonged to 2 h, the increased extents were decreased to 2.92-fold and 1.13-fold, respectively. Increase of choline and ethanolamine could contribute to PC synthesis. These results suggest that PC synthesis was enhanced by *p*-HPCD stress.

In order to further determine increase of phospholipids biosynthesis, we conducted thin layer chromatography (TLC) to quantify phospholipids in *p*-HPCD treated and non-treated cells. Extracted lipids corresponding to 5.2×10^7 cells of each sample were analyzed. As shown in Fig. 7, after 2 h the level of phospholipid components (PE, PI and PC) in the *p*-HPCD treated cells was detected to be elevated

compared to non-treated control cells. From these results, it is confirmed that phospholipid biosynthesis was induced by *p*-HPCD stress.

Table 8. Relative concentrations of metabolites involving polyamines and phospholipid after *p*-HPCD treatment for 1 h and 2 h, respectively.

Metabolite Name	1 h			2 h		
	Relative peak area		Relative concentration	Relative peak area		Relative concentration
	Control	Treated	Fold-change	Control	Treated	Fold-change
Choline	0.106	0.464	4.37	0.225	0.658	2.92
GABA	0.002	0.007	3.33	0.003	0.013	3.87
Spermidine	0.010	0.030	3.09	0.016	0.047	2.99
Putrescine	0.003	0.008	2.88	0.003	0.011	3.55
N-Acetylputrescine	0.017	0.029	1.74	0.016	0.038	2.31
Glycerophosphocholine	1.018	1.743	1.71	1.730	2.889	1.67
Ethanolamine	0.128	0.208	1.63	0.176	0.200	1.13
S-Adenosylmethionine	0.035	0.044	1.27	0.046	0.081	1.74

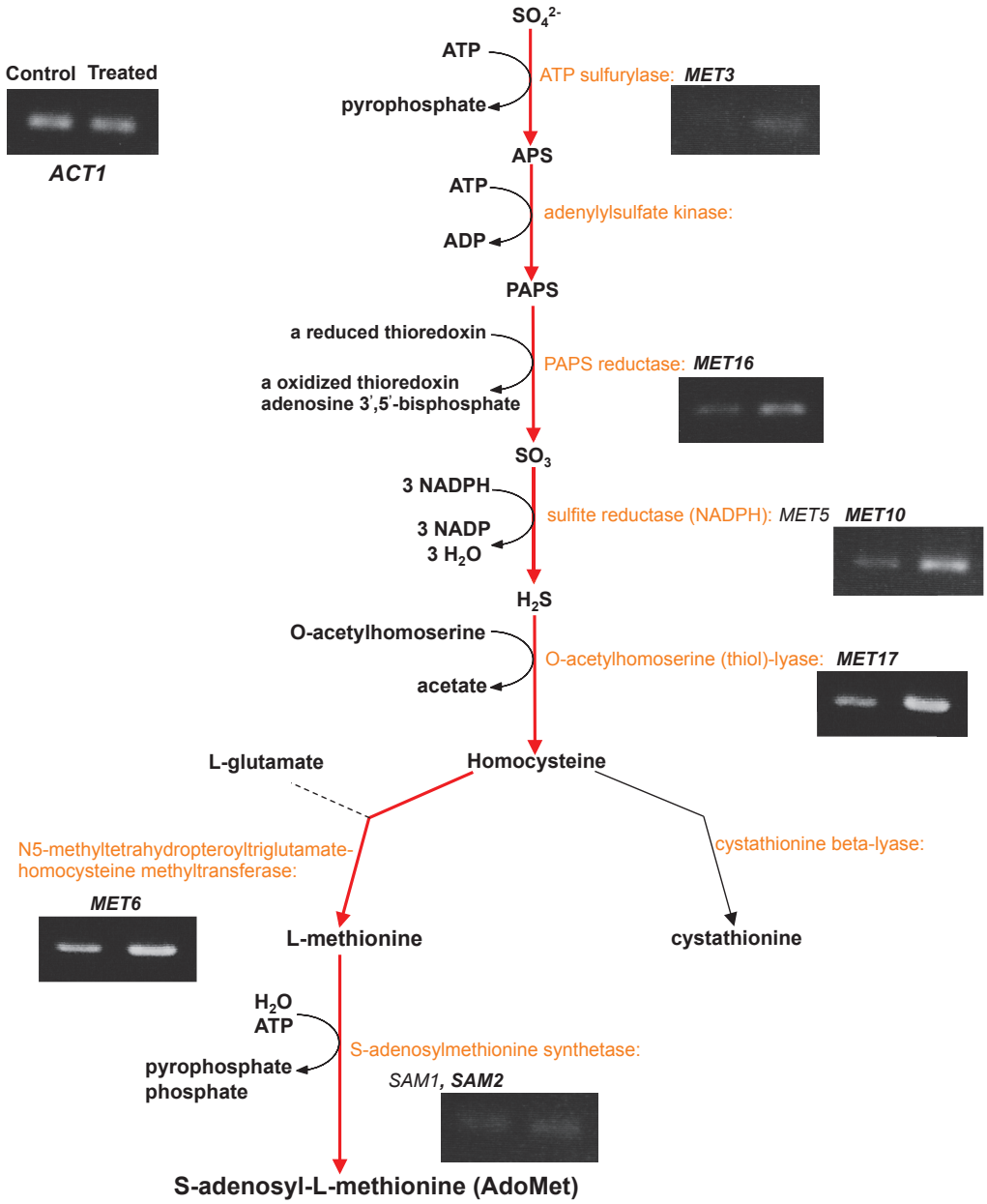

Fig. 5. *S*-adenosyl-L-methionine (AdoMet) biosynthesis pathway in yeast. Transcriptional levels of related genes were evaluated by RT-PCR using *ACT1* gene as the reference gene. Induced genes are shown in bold and italic.

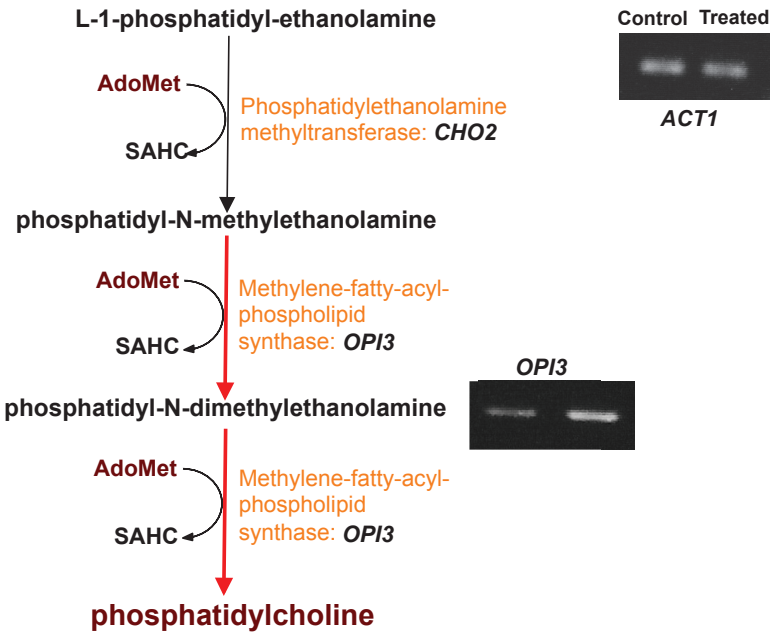

Fig. 6. Phosphatidylethanolamine methylation pathway of phosphatidylcholine biosynthesis in yeast. Transcriptional level of key gene *OPI3* was evaluated by RT-PCR using *ACT1* gene as the reference gene.

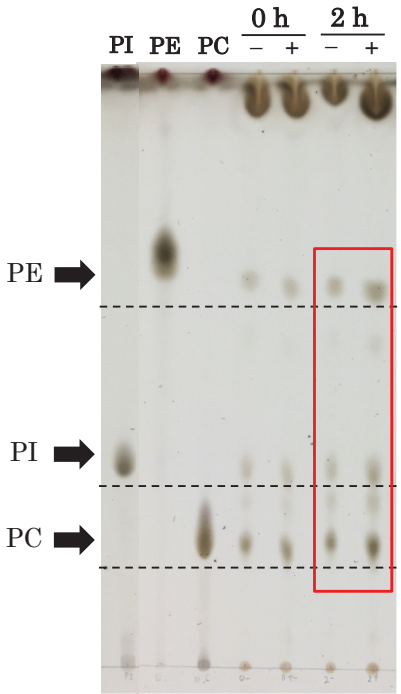

Fig. 7. Quantification of phospholipid components in treated and non-treated yeast cells using thin layer chromatography (TLC). Phospholipids PI, PE and PC were used as standards.

3.8 Amounts of most of amino acids involving protein synthesis were decreased after *p*-HPCD treatment

Fig. 8 shows relative concentrations of amino acids involving protein synthesis after *p*-HPCD treatment for 1 h and 2 h. Level of each amino acid was calculated relative to control. Amounts of six amino acids (Lys, Ser, Gly, Ala, ßAla and Leu) showed increased after treatment for 1 h, while their relative concentrations their increased extents showed decreased as a function of prolonging treated time to 2 h. After *p*-HPCD treatment for 2 h, there are 66.7% of amino acids highly decreased, especially glutamate family (Glu, Gln, Arg, Pro and Lys) and aromatic family (His, Phe, Tyr and Trp) relative to control. Among these amino acids, glutamate and glutamine play important roles in biosynthesis of nitrogenous compounds. In *S.cerevisiae*, ~85% of the total cellular nitrogen is incorporated via the amino nitrogen of glutamate and ~15% are derived from the amide group of glutamine [27]. However, levels of glutamate and glutamine were decreased by 0.53-fold and 0.83-fold after 2 h treatment of *p*-HPCD relative to control. Because YPD is a rich complex medium that contains sufficient nutrients required for yeast growth, uptake of amino acids from medium was probably impeded under *p*-HPCD condition. Most of molecules are transported into cellular interior with a carrier protein on membrane. Change of membrane structure indicates the change of selective permeability of membrane [28].

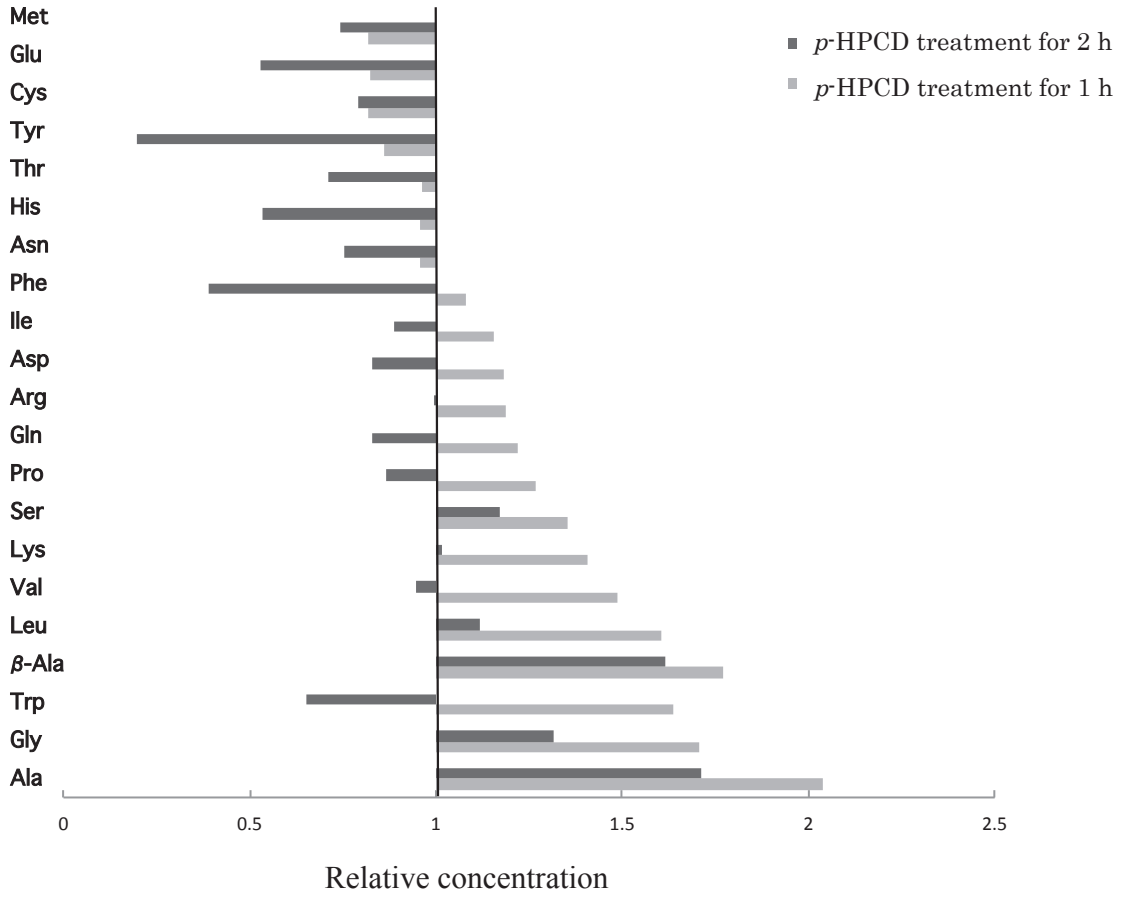

Fig. 8. Relative concentrations of amino acids involving protein synthesis after *p*-HPCD treatment for 1 h and 2 h, respectively.

3.9 Morphological modification of cell surface was observed after *p*-HPCD treatment

To visually observe cell changes, scanning electron microscope (SEM) was used to inspect surface changes induced by 0.5 MPa, 1.0 MPa, 2.0 MPa and 4.0 MPa of CO_2 for 3 h treatment. The appearance of dimple was recognized on cell surface (Fig. 9B, C and D). We took micrographs of four randomly selected areas at 3000-fold and then counted all cells and cells with dimple without regard to dimple size. Cell viability and percentages of cells with dimple are shown in Fig. 10. The percentage was calculated by $N_d / N_t \times 100\%$ (N_d: number of cell with dimple; N_t: total number of cell). Before CO_2 treatment, a small portion of dimpled cells (5.3%) was observed (Fig. 9A), which is thought as a result of ethanol dehydration treatment before SEM inspection. However, with CO_2 pressure increasing, the percentage of cell with dimple showed significantly increased relative to non-treated sample. Cell surface morphology was also inspected after 3.0 MPa of CO_2 for 4 h, 6 h, 8 h, 12 h and 16 h treatment (Fig. 9E). The percentage of irregular cell surface with dimple increased with the treated time extending (Fig. 11). In addition to induction of genes involved in phospholipid biosynthesis, DNA microarray analysis also revealed that expression of genes related to synthesis of cell wall components (mannoproteins and chitin) and cell wall architecture increased after *p*-HPCD treatment (Table 9). It seems that CO_2 with high concentration makes morphological changes on cell surface easier to occur during ethanol dehydration treatment; in other words, SEM observations confirmed that stability of membrane structure was disturbed by CO_2.

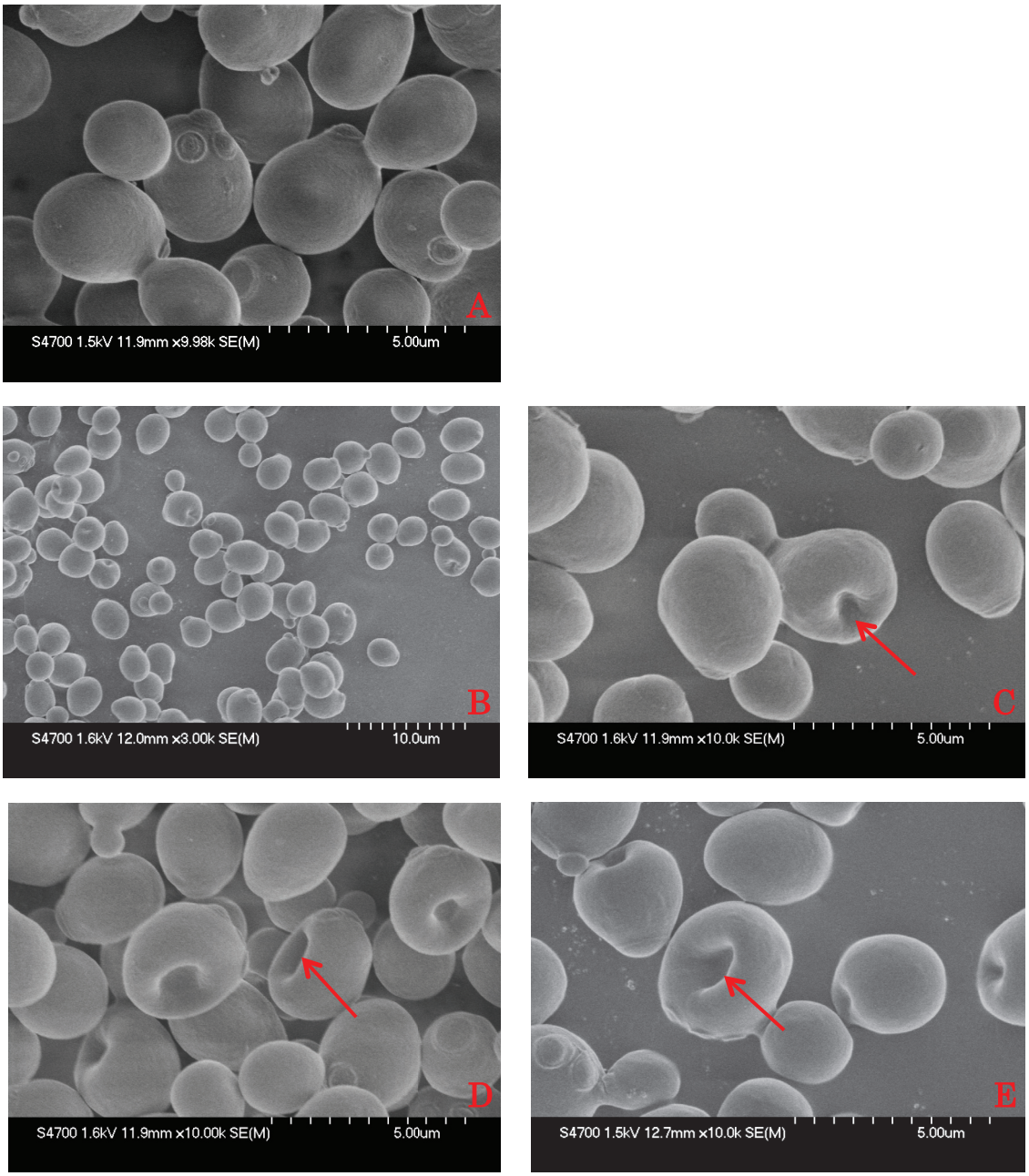

Fig. 9. Scanning electron micrographs before (A) and after pressurized CO_2 treatment. Micrographs B and C show yeast cells after 1.0 MPa of CO_2 for 3 h treatment at 3000-fold and 10000-fold, respectively. Micrograph D shows yeast cells after 4.0 MPa of CO_2 for 3 h treatment at 10000-fold. Micrograph E shows yeast cells after 3.0 MPa of CO_2 for 4 h treatment at 10000-fold.

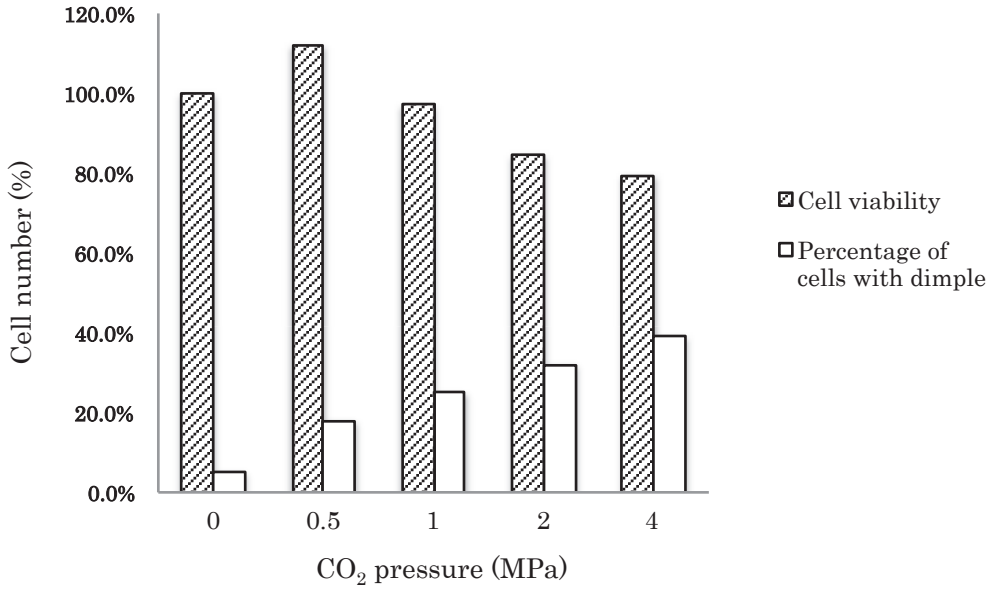

Fig. 10. Cell viability and percentages of cells with dimple after 0.5 MPa, 1.0 MPa, 2.0 MPa and 4.0 MPa of CO_2 for 3 h treatment.

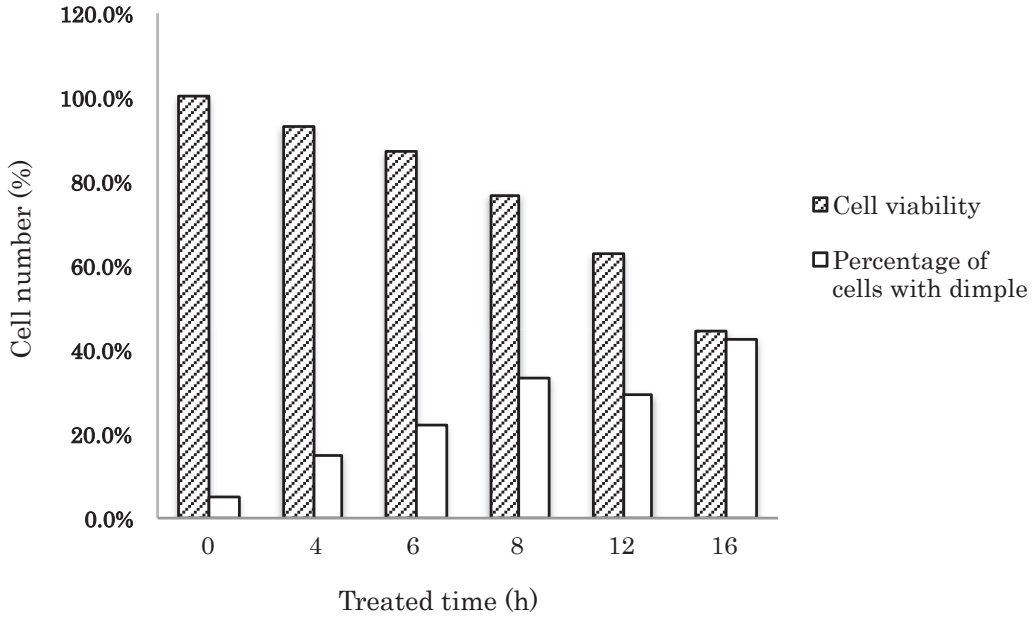

Fig. 11. Cell viability and percentages of cells with dimple after 3.0 MPa of CO_2 for 4 h, 6 h, 8 h, 12 h and 16 h treatment.

Table 9. Induced genes associated with cell wall biogenesis and architecture. Cy5/Cy3 ratio indicates the normalized expression ratio of Cy5 (*p*-HPCD treatment for 2 h) and Cy3 (control) obtained from DNA microarray [16].

Gene Name	Cy5/Cy3 Ratio	Function
FIT2	**22.8**	Mannoprotein incorporated into the cell wall via a GPI[a] anchor
FIT3	**13.4**	Mannoprotein incorporated into the cell wall via a GPI[a] anchor
ECM4	**5.4**	Glutathione transferase involved in the cell-surface biogenesis and architecture
FIT1	**4.7**	Mannoprotein incorporated into the cell wall via a GPI[a] anchor
SPS100	**4.6**	Sporulation-specific wall maturation protein
SHC1	**3.2**	Sporulation-specific activator of Chs3p (chitin synthase III)
ECM8	**2.9**	Protein with unknown function that may involve in cell wall structure or biosynthesis
WSC3	**2.5**	Sensor transducer involved in maintenance of cell wall integrity
CCW14	**2.3**	Covalently linked cell wall glycoprotein
ECM30	**2.1**	Protein with unknown function that may involve in cell wall biosynthesis
MPT5	**2.1**	mRNA-binding protein of the PUF family that has a role in maintenance of cell wall integrity

[a] GPI: glycosylphosphatidylinositol.

4. DISCUSSION

4.1 Metabolism of urea cycle is enhanced in response to *p*-HPCD stress

In YPD medium with high water content, CO_2 can dissolve to form carbonic acid (H_2CO_3), which further dissociates into bicarbonate (HCO_3^-), carbonate (CO_3^{2-}) and hydrogen (H^+) ionic species according to the following equilibriums:

$$CO_2 + H_2O \Leftrightarrow H_2CO_3 \quad (1)$$

$$H_2CO_3 \Leftrightarrow HCO_3^- + H^+ \quad (2)$$

$$HCO_3^- \Leftrightarrow CO_3^{2-} + H^+ \quad (3)$$

Under homothermal condition, a higher pressure significantly enhances solubility of CO_2 in unsaturated solutions [29]. It is presumed that CO_2 or HCO_3^- under higher pressure can penetrate through cell membrane and accumulate in the cellular interior. The applied CO_2 pressure may convert HCO_3^- to CO_3^{2-}, which could precipitate intracellular inorganic electrolytes (such as Ca^{2+}, Mg^{2+} and similar ions) from cells and cell membranes. These inorganic electrolytes help to maintain the osmotic homeostasis, thus their precipitation could disorder inorganic electrolytes balance, which has harmful effects on the cell volume [30]. The urea cycle, also known as ornithine cycle, is a cycle of biochemical reactions occurring in many organisms. As Fig. 12 shown, the synthesis of urea in yeast cells requires two amino groups from NH_4^+ and aspartate, and one carbon atom from HCO_3^-. The induction of urea cycle metabolism could increase the utilization of HCO_3^- and facilitate to remove redundant HCO_3^-, thereby decrease production of CO_3^{2-}. Moreover, liberation of H^+ ion could be decreased along with the inhibition of HCO_3^- dissociation. Although yeast cell has mechanism of controlling and regulating intracellular pH, such as cytoplasmic

buffering and proton pumps [31], increased energy consumption to maintain pH homeostasis by the proton motive force may diminish cell resistance to inactivation.

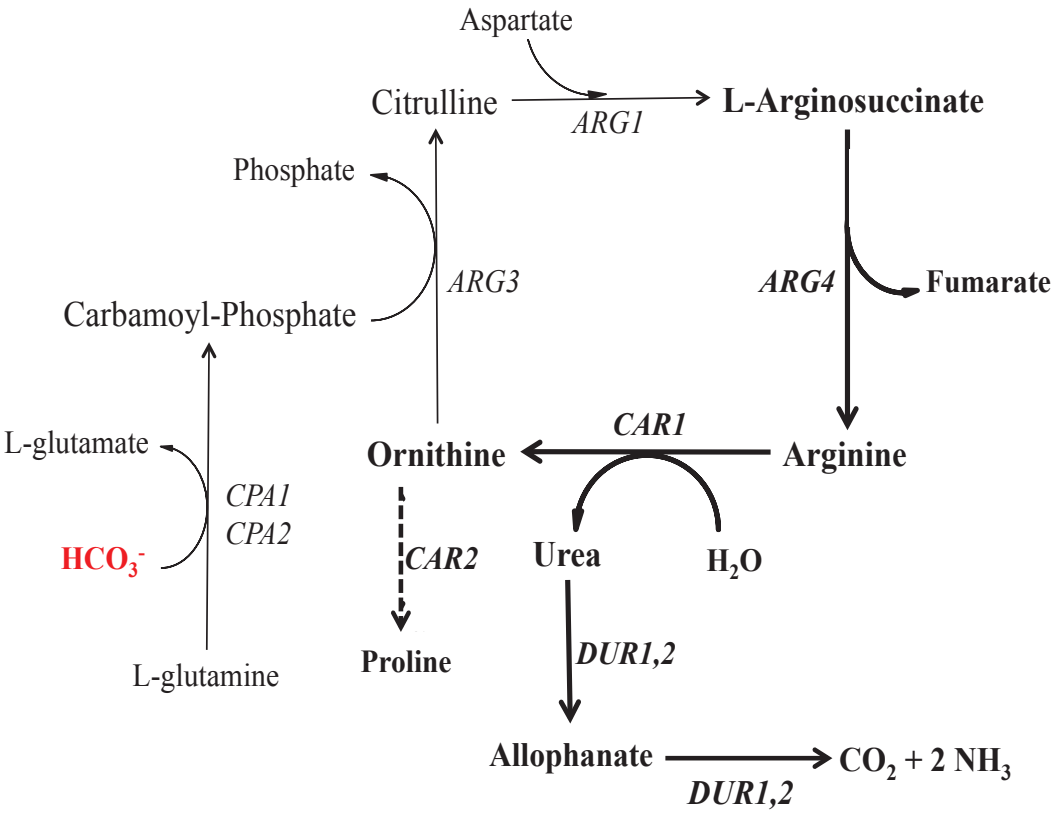

Fig. 12. Urea cycle pathway in brief.

Note: The induced genes and relevant metabolic pathway are shown in bold.

4.2 *P*-HPCD stress induces structural and functional disorders of cell membrane

The biological membrane as a basis for HPCD-mediated growth inhibition has been implicated in the past years. In aqueous solution, the hydration equilibrium constant and two dissociation constants of carbonic acid are quite small (at 25℃). Hence, the majority of CO_2 remains as CO_2 molecules. When a concentration gradient exists on the two sides of membrane, CO_2 can passively move across membrane by diffusion and could accumulate into the lipophilic inner layer [32]. Spilimbergo et al. theoretically confirmed high affinity between CO_2 and plasma membrane and calculated that CO_2 can be dissolved in the phospholipids of a cell membrane model at a very great extent [3]. When the lipid phase of a membrane is occupied by foreign molecules, the fluidity of the membrane could be changed [33]. The accumulated CO_2 in the lipid phase may structurally and functionally disorder cell membrane due to an order loss of the lipid chains. Additionally, it is considered that optimum membrane function not only requires optimum fluidity but an optimum surface charge density [34]. Researchers proposed that HCO_3^- ion may have an influence on the charged phospholipid head groups and membrane proteins to alter the charge density of cell surface, thereby altering optimal membrane-mediated functions, e.g. regulation of passive, facilitated and active fluxes, membrane fusion, destructure of essential membrane domains, and other vital functions. The effects of both CO_2 (aqueous) and HCO_3^- on membrane could be the most likely reasons for the decreased growth rate of yeast.

Unfortunately, previous researches on yeast membrane response to CO_2 exposure did not study the response of phospholipid. In our study, through DNA

microarray and metabolomic analysis, we found that *p*-HPCD stress induces AdoMet synthesis, which contributes to enhance PC synthesis. PC is the most abundant phospholipid present in the membranes of eukaryotic cells. Being a major structural component of cell membranes, PC plays an essential role in maintaining membrane permeability barriers [35]. Moreover, it is demonstrated that PC has a cylindrical shape with similar cross-sectional areas for head group and acyl chains of the molecule and prefers to assemble into a bilayer, which makes it better suited to maintain membrane integrity [36]. The enhancement of PC synthesis is very likely to maintain optimum structure and functions of cell membrane so that cell resistance to inactivation under *p*-HPCD treatment could be improved.

The *p*-HPCD treatment seems to be a very promising alternative pasteurization technology. To meet these high expectations, however, clear, objective and bias data and information about pasteurization mechanism and improvements this technique represents are needed to convince consumers and stakeholders. In this study, under *p*-HPCD-induced growth-inhibitory condition, we confirmed disturbance of cell membrane; what's more, the response of a major membrane component (PC) was also found out. Besides cell membrane, *p*-HPCD stress could exert effects on cellular membranous organelles as well.

5. CONCLUSION

This study focused on exploring growth-inhibitory mechanism of *p*-HPCD pasteurization technology by analyzing the transcriptional responses of yeast cell through functional genomics as well as cluster analysis, and by measuring cellular metabolites changes through metabolomics. Growth inhibition of yeast cell could result from disorder of inorganic electrolytes balance and disturbance of cell membrane structure and function. The induction of urea cycle metabolism and phospholipid biosynthesis in response to *p*-HPCD stress seems to play important roles in cell survival. Our study provides some directions for future research towards elucidating the exact pasteurization mechanism of *p*-HPCD technology, which would contribute to promote its rapid development in food industry.

6. ACKNOWLEDGEMENT

This work was supported by JSPS KAKENHI Grant Number JP23580191.

I would like to thank Dr. Hitoshi Iwahashi of Gifu University in Japan for giving me an opportunity to study in his laboratory. I must thank for his valuable suggestions and guidance.

I'm also thankful to Prof. Katsuhiro Tamura, Prof. Yoshihisa Suzuki, Dr. Satoshi Kawachi and Mr. Hiroyuki Matsuoka for sharing their technical and scientific knowledge without any reservation to conduct this research.

I also express thank to Dr. Kazuki Nomura and other students in Applied Microbiology Laboratory of Gifu University for their earnest help.

7. REFERENCE

[1] D. Durance,T.(1997). Improving canned food quality with variable retort temperature processes, Trends Food Sci.Tecnol. 8:113–118.

[2] Ortega-Rivas,E. and Salmerón-Ochoa,I.(2012). Nonthermal Food Processing Alternatives and Their Effects on Taste and Flavor Compounds of Beverages. Crit. Rev. Food Sci. 54(2):190–207.

[3] Valley,G. and Rettger,L.F.(1927). The influence of carbon dioxide on bacteria. J. Bacteriol. 14(2):101–137.

[4] Fraser,D.(1951). Bursting bacteria by release of gas pressure. Nature. 167:33–34.

[5] Zhang,J., Davis,T.A., Matthews,M.A., Drews,M.J., LaBerge,M., An,Y.H.(2006). Sterilization using high-pressure carbon dioxide. J. of Supercritical Fluids. 38:354–372.

[6] Garcia-Gonzalez,L., Geeraerd,A.H., Spilimbergo,S., Elst,K., Van Ginneken,L., Debevere,J., Van Impe,J.F., Devlieghere,F.(2007). High pressure carbon dioxide inactivation of microorganisms in foods: The past, the present and the future. Int. J. Food Microbiol. 117(1):1–28.

[7] Harada,N., Iwahashi,H., Obuchi,K., Tamura,K.(2008). Effect of *petit*-high pressure sterilization for fruit juice investigation for long time treatment with *Petit*-High Pressure Carbon Dioxide gas. In: Abe F, editor. Proceedings of the 15th Symposium for Japanese Research Group of High Pressure Bioscience and Biotechnology, pp. 96–100.

[8] Dillow,A.K., Dehghani,F., Hrkach,J.S., Foster,N.R., Langer,R.(1999). Bacterial inactivation by using near- and supercritical carbon dioxide. Proceedings of the National Academy of Sciences of the United States of America, 96,10344–10348.

[9] Foster,J.W., Cowan,R.M., Maag,T.A.(1962). Rupture of bacteria by explosive decompression, J. Bacteriol. 83(2):330–334.

[10] Enomoto,A., Nakamura,K., Nagai,K., Hashimoto,T., Hakoda,M.(1997). Inactivation of food microorganisms by high-pressure carbon dioxide treatment with or without explosive decompression, Biosci. Biotechnol. Biochem. 61(7):1133–1137.

[11] Nakamura,K., Enomoto,A., Fukushima,H., Nagai,K., Hakoda,M.(1994). Disruption of Microbial Cells by the Flash Discharge of High-pressure Carbon Dioxide. Biosci. Biotech. Biochem. 58(7):1297–1301.

[12] Budisa,N. and Schulze-Makuch,D.(2014). Supercritical Carbon Dioxide and Its Potential as a Life-Sustaining Solvent in a Planetary Environment. Life. 4,331–340.

[13] Yasokawa,D. and Iwahashi,H.(2010). Toxicogenomics using yeast DNA microarrays. J. Biosci. Bioeng. 110(5):511–522.

[14] Gasch,A.P., Spellman,P.T., Kao,C.M., Carmel-Harel,O., Eisen,M.B., Storz,G., Botstein,D., Brown,P.O.(2000). Genomic expression programs in the response of yeast cells to environmental changes. Mol. Biol. Cell. 11(12):4241–4257.

[15] Jordan,K.W., Nordenstam,J., Lauwers,G.Y., Rothenberger,D.A., Alavi,K., Garwood,M., Cheng,L.L.(2009). Metabolomic Characterization of Human Rectal Adenocarcinoma with Intact Tissue Magnetic Resonance Spectroscopy. Dis. Colon. Rectum. 52 (3):520–525.

[16] Matsuoka,H., Suzuki,Y., Iwahashi,H., Arao,T., Suzuki,Y., Tamura,K.(2005). The biological effects of high-pressure gas on the yeast transcriptome. Braz. J. Med. Biol. Res. 38(8):1267–1272.

[17] Bligh,E.G. and Dyer,W.J.(1959). A rapid method of total lipid extraction and purification. Can. J. Biochem. Physiol. 37:911–917.

[18] Park,H.D., Scott,S., Rai,R., Dorrington,R., Cooper,T.G.(1999). Synergistic operation of the CAR2 (Ornithine transaminase) promoter elements in *Saccharomyces cerevisiae*. J. Bacteriol. 181(22):7052–7064.

[19] van Vuuren,H.J., Daugherty,J.R., Rai,R., Cooper,T.G.(1991). Upstream induction sequence, the cis-acting element required for response to the allantoin pathway inducer and enhancement of operation of the nitrogen-regulated upstream activation sequence in *Saccharomyces cerevisiae*. J. Bacteriol. 173(22):7186–7195.

[20] Sirisattha,S., Momose,Y., Kitagawa,E., Iwahashi,H.(2004). Toxicity of anionic detergents determined by *Saccharomyces cerevisiae* microarray analysis, Water Res. 38(1):61–70.

[21] Sirisattha,S., Momose,Y., Kitagawa,E., Iwahashi.H.(2004). Genomic profile of roundup treatment of yeast using DNA microarray analysis, Environ. Sci. 11(6):313–323.

[22] Helenius, A. and Simons, K. (1975). Solubilization of membranes by detergents. Biochim. Biophys. Acta. 415:29–79.

[23] Li,S.P., Tang,T.S., Yiu,K.S., Lo,K.K.(2012). Cyclometalated iridium(III)-polyamine complexes with intense and long- lived multicolor phosphorescence: synthesis, crystal structure, photophysical behavior, cellular uptake, and transfection properties, Chemistry 18:13342–13354.

[24] Thomas,D. and Surdin-Kerjan,Y.(1997). Metabolism of sulfur amino acids in *Saccharomyces cerevisiae*, Microbiol. Mol. Biol. Rev. 61(4):503–532.

[25] Tehlivets,O., Malanovic,N., Visram,M., Pavkov-Keller,T., Kellera,W.(2013). S-adenosyl-L-homocysteine hydrolase and methylation disorders: Yeast as amodel system, Biochim. Biophys. Acta 1832(1):204–215.

[26] Dowd,S.R., Bier,M.E., Patton-Vogt,J.L.(2001). Turnover of phosphatidylcholine in *Saccharomyces cerevisiae*. The role of the CDP-choline pathway, J. Biol. Chem. 276(6):3756–3763.

[27] Ljungdahl,P.O. and Daignan-Fornier,B.(2012). Regulation of Amino Acid, Nucleotide, and Phosphate Metabolism in *Saccharomyces cerevisiae*. Genetics. 190(3):885–929.

[28] Ek-Vitorin,J.F. and Burt,J.M.(2013). Structural basis for the selective permeability of channels made of communicating junction proteins, BBA-Biomembranes 1828 (1):51–68.

[29] Duan,Z.H. and Sun,R.(2003). An improved model calculating CO_2 solubility in pure water and aqueous NaCl solutions from 273 to 533 K and from 0 to 2000 bar. Chem. Geol. 193(3-4):257–271.

[30] Lin,H.M., Yang,Z.Y., Chen,L.F.(1993). Inactivation of Leuconostoc dextranicum with carbon dioxide under pressure. The Chem. Eng. J. 52(1):B29–B34.

[31] Hutkins,R.W.and Nannen,N.L.(1993). pH homeostasis in Lactic acid bacteria. J. Dairy Sci. 76(8):2354–2365.

[32] Isenschmid,A., Marison,I.W., von Stockar,U.(1995). The influence of pressure and temperature of compressed CO_2 on the survival of yeast cells, J. Biotechnol. 39(3):229–237.

[33] Pang,K.Y., Braswell,L.M., Chang,L., Sommer,T.J., Miller,K.W.(1980). The perturbation of lipid bilayers by general anesthetics: a quantitative test of the disordered lipid hypothesis, Mol. Pharm. 18(1):84–90.

[34] Jones,R.P. and Greenfield,P.F.(1982). Effect of carbon dioxide on yeast growth and fermentation, Enzym. Microb. Technol. 4(4):210–223.

[35] Boumann,H.A., Gubbens,J., Koorengevel,M.C., Oh,C.S., Martin,C.E., Heck,A.J., Patton-Vogt,J., Henry,S.A., de Kruijff,B., de Kroon,A.I.(2006). Depletion of phosphatidylcholine in yeast induces shortening and increased saturation of the lipid acyl chains. Evidence for regulation of intrinsic membrane curvature in a eukaryote, Mol. Biol. Cell 17,1006–1017.

[36] Allison,D. and Roland,F.(2008). Examining the contributions of lipid shape and headgroup charge on bilayer behavior, Biophys. J. 95(6):2636–2646.